

Influence of band structure effects on domain-wall resistance in diluted ferromagnetic semiconductors

R. Oszwałdowski,¹ J. A. Majewski,² and T. Dietl³

¹*Institute of Physics, Nicolaus Copernicus University, Grudziądzka 5, PL 87-100 Toruń, Poland*

²*Institute of Theoretical Physics, Warsaw University, PL 00-681 Warszawa, Poland*

³*Institute of Theoretical Physics, Warsaw University, PL 00-681 Warszawa, Poland*

*Institute of Physics, Polish Academy of Sciences and ERATO Semiconductor Spintronics
Project of Japan Science and Technology Agency, PL 02-668 Warszawa, Poland*

(Dated: July 3, 2018)

Intrinsic domain-wall resistance (DWR) in (Ga,Mn)As is studied theoretically and compared to experimental results. The recently developed model of spin transport in diluted ferromagnetic semiconductors [Van Dorpe *et al.*, Phys. Rev. B **72**, 205322 (2005)] is employed. The model combines the disorder-free Landauer-Büttiker formalism with the tight-binding description of the host band structure. The obtained results show how much the spherical 4×4 $\mathbf{k}\mathbf{p}$ model [Nguyen, Shchelushkin, and Brataas, cond-mat/0601436] overestimates DWR in the adiabatic limit, and reveal the dependence of DWR on the magnetization profile and crystallographic orientation of the wall.

PACS numbers: 75.47.Jn, 72.25.Dc, 75.50.Pp

Recently, current-induced domain-wall displacement¹ and intrinsic domain-wall resistance^{2,3} have been observed in ferromagnetic semiconductor (Ga,Mn)As. These results attract a great deal of attention as they address the question of spin dynamics in the presence of spatially inhomogeneous magnetization texture as well as open the doors for novel concepts of high-density memories and logic devices.

Since in (Ga,Mn)As the domain-wall (DW) width $\pi\lambda_W \sim 20$ nm is much longer than the mean free path $\ell \sim 0.5$ nm, it has been found³ that disorder, inherent to carrier-controlled ferromagnetic semiconductors, plays an essential role in determining the magnitude of intrinsic domain-wall resistance (DWR). It can be expected that band structure effects, particularly the spin-orbit interaction, which accounts for magnetoelastic^{4,5} and magnetotransport⁶ properties of these materials, also affect the DWR. Indeed, according to recent work of Nguyen, Shchelushkin, and Brataas,⁷ in the presence of the valence-band splitting into light and heavy hole subbands, DWR remains non-zero even in the absence of disorder and in the adiabatic limit, $\pi\lambda_W \gg \lambda_F$, where λ_F is the Fermi wavelength. This conclusion, obtained within the 4×4 Luttinger model, questions the generality of the time-honored result of Cabrera and Falicov,⁸ who showed that the transition probability of the quantum spin through a DW approaches 1 in the adiabatic limit.

In this paper we implement multi-orbital tight-binding (TB) Hamiltonian into the Landauer-Büttiker formalism for spin-dependent quantum transport in the ballistic regime. The TB method is known to be more universal than $\mathbf{k}\mathbf{p}$ approaches. It successfully describes small quantum dots and heterojunctions between materials with different band structures. This comes at the cost of a limit to size of the studied system. We find, however, that this limitation is not prohibitive in the case we study here. Actually, a variant of this theory was already applied to describe the spin polarization of electron cur-

rent in the (Ga,Mn)As/n-GaAs Esaki-Zener diodes^{9,10} as well as to successfully evaluate the magnitude of TMR in (Ga,Mn)As/GaAs/(Ga,Mn)As trilayer structures.¹⁰

In this work we determine the magnitude of DWR for various domain-wall widths, shapes, and crystallographic orientations. In particular, we find out to what extent the 4×4 spherical Luttinger model,⁷ known to overestimate the effect of the spin-orbit interaction for the relevant values of Fermi energies,⁵ overvalues the magnitude of DWR in the adiabatic limit. Furthermore, we reveal the dependence of DWR on the crystallographic orientation of the DW, an effect not studied so far. Finally, we compare results of our disorder-free theory to experimentally determined values of DWR.

The transmission matrix employed here is determined in terms of the extended transfer-matrix method¹¹ within the TB approach, with the spin-orbit coupling included. The (Ga,Mn)As valence-band structure for small Mn content was shown to be similar to that of GaAs.¹² Thus we use sp^3s^* parameters proposed for GaAs.¹³ This model reproduces correctly the band structure of GaAs in the relevant part of the Brillouin zone. Moreover, it takes into account the Dresselhaus terms, essential for the spin-dependent transport.

The presence of the Mn ions and, therefore, of the sp-d exchange interaction, is introduced to the TB Hamiltonian using the virtual crystal and mean-field approximations, taking into account the appropriate weights of Ga and As orbitals in the wavefunctions close to the center of the Brillouin zone.^{5,14} For the Mn content of 5% the hole subband splitting at the Γ point obtained by the present method is 150 meV and 46 meV for the heavy and light holes respectively, which compares favorably with the $\mathbf{k}\mathbf{p}$ values of 150 and 50 meV.⁵ In what follows we use h_0 as a measure of magnetization, where $3h_0$ is the heavy-holes splitting, and $h_0/2 = B_G$, where B_G is the splitting parameter of Ref. 5.

To study coherent transport through the DW we de-

fine three regions along the current direction: left and right leads, and a central multi-layer region of the length $L_0 \gg \lambda_W$ containing the DW, where L_0 , taken here to be 40 nm, can be identified as the phase coherence length of the system, $L_0 \approx L_\varphi(T)$. The Mn concentration is constant throughout the three sections. In the central region magnetization \mathbf{M} rotates, so that its deviation θ from the initial orientation [001], taken here as the z -direction, changes by small steps in the consecutive atomic layers, according to $\cos\theta = \tanh(x/\lambda_W)$, where x is the distance from the DW center in the current direction. We consider the Bloch and the Néel DWs,¹⁵ for which the vector $\mathbf{M}(0) \times \mathbf{M}(\theta)$ is along the current direction or perpendicular to it, respectively. In addition to 180° walls we study a 90° Bloch DW, for which the magnetization in the left lead is normal to the \mathbf{M} direction in the right lead. Since the virtual crystal approximation restores translational invariance in the direction perpendicular to the current, we model the lateral extent of the system by Born-von Karman boundary conditions. We assume no strain in the entire structure.

In our calculations, we place the Fermi level E_F at either 0.08 eV, 0.2 eV, or 0.36 eV below the mid-point of the heavy and light hole bands at the Γ point, thus covering the experimentally relevant hole concentration range, as $p = 1 \times 10^{20} \text{ cm}^{-3}$, $3.5 \times 10^{20} \text{ cm}^{-3}$, and $1 \times 10^{21} \text{ cm}^{-3}$, respectively. In order to produce a non-zero current density, we introduce a bias V by shifting the Fermi level of the right lead with respect to the left one. The bias value $\sim 10^{-4}$ eV is much smaller than typical splitting in the valence band, so that the calculated resistances are bias-independent. We obtain the current density from the transmission coefficients by energy integration over the range from $E_F - eV$ to E_F and summation over \mathbf{k}_\parallel vectors over a two-dimensional grid.¹⁶ We find that typically grids of 200 k -points are sufficient, except for more subtle problems, such as that of adiabatic passage (Fig. 3), which required a 550 k -point grid. Using the current density and the bias we obtain the total resistance R_T of the structure containing the DW, in units $\Omega\mu\text{m}^2$. We define DWR as a difference between R_T and the resistance for the uniform magnetization in the whole structure. Since disorder is neglected, the latter corresponds to the Sharvin resistance R_S , as all accessible channels are fully transmitting for spatially homogeneous magnetization.

Figure 1 depicts DWR obtained within our sp^3s^* TB model for $h_0 = 50$ meV. We consider current flowing in either $[\bar{1}10]$ or $[100]$ directions, while \mathbf{M} in the left (right) lead is parallel (anti-parallel) to the $[001]$ direction. We present relative resistance of the DW, which is defined as $R_r = (R_T - R_S)/R_S$. In Fig. 1 the DW width λ_W is given in units of the Fermi wavelength λ_F of the heavy holes for \mathbf{k}_F in the $[100]$ direction in the absence of magnetization ($h_0 = 0$). This corresponds to $\lambda_F = 5.7$ and 3.7 nm for $p = 10^{20}$ and $3.5 \times 10^{20} \text{ cm}^{-3}$, respectively. The value $\lambda_W = 0$ denotes a step-like DW profile.

We see in Fig. 1(a) that in the adiabatic limit, $\lambda_W \gtrsim \lambda_F$, the relative resistance R_r saturates and remains non-

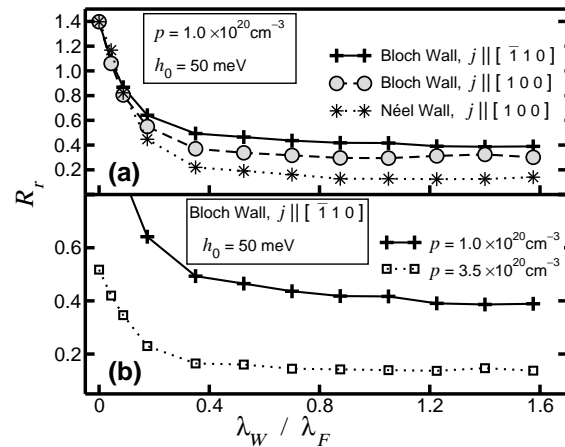


FIG. 1: (a) The predicted relative domain-wall resistance R_r for (Ga,Mn)As as a function of the DW width parameter λ_W (in units of the Fermi wavelength $\lambda_F = 5.7$ nm) for various current directions and domain-wall profiles. (b) R_r for two hole densities $p = 1 \times 10^{20} \text{ cm}^{-3}$ and $p = 3.5 \times 10^{20} \text{ cm}^{-3}$.

zero. The range $\lambda_W > \lambda_F$ is relevant for experiments with typical (Ga,Mn)As films.

Some residual variations of R_r in this region are probably caused by Fabry-Perot-like interference that occurs for a finite L_0 . At the same time, according to the results depicted in Fig. 1(b), the magnitude of R_r becomes significantly smaller for higher values of the hole density. Furthermore, R_r for the Néel wall is seen to be substantially lower than for the Bloch wall (Fig. 1(a)). These findings confirm results obtained by Nguyen, Shchelushkin, and Brataas,⁷ though our more complete theory leads to R_r up to a factor of two smaller than that resulting from the spherical 4×4 model. This can be seen for example in Fig. 1(b), where the lower curve corresponds to $h_0/E_F = 0.23$. In this case our TB-based model predicts $R_r \approx 0.14$, while the $\mathbf{k}\mathbf{p}$ one yields almost 0.3. Moreover, we find that the magnitude of R_r varies significantly with the DW orientation (Fig. 1(a)). This effect results from the dependence of R_T on the crystallographic directions of the current and magnetization.

To elucidate the origin of the non-zero DWR in the adiabatic limit, we have repeated our calculations switching off the spin-orbit coupling. Thus, we take entire complexity of the valence band into account except for putting the spin-orbit parameters λ^a and λ^c of the TB Hamiltonian equal to zero in the whole structure. As shown in Fig. 2, R_r no longer saturates but instead vanishes with λ_W/λ_F , a behavior first noted by Cabrera and Falicov,⁸ for the free electron case. In the case of $[\bar{1}10]$ direction the R_r exhibits certain deviation from the expected exponential drop. We ascribe this behavior to the presence of grazing incidence channels for which the \mathbf{k} component along the current direction is small, so that the reflection coefficient is still relatively high.⁸ We conclude that non-zero DWR of (Ga,Mn)As in the adiabatic limit originates from the spin-orbit coupling rather than from multiband

transport in the valence band. This substantiates the previous suggestion,⁷ put forward by noting that DWR vanishes if 4×4 Luttinger Hamiltonian is assumed to be diagonal. In this case and in the thick-wall limit, the spin of the carrier can adiabatically track the local magnetization and the charge transport is not affected by the presence of DW.^{8,17}

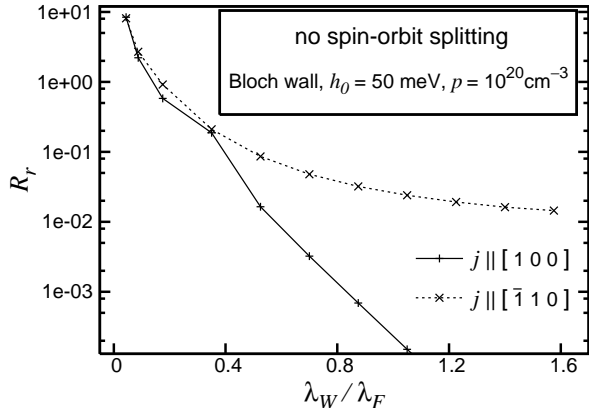


FIG. 2: The theoretical predictions of intrinsic domain-wall resistance in the absence of the spin-orbit coupling. In the case of the domain wall normal to $[1 0 0]$, the relative domain-wall resistance (R_r) drops exponentially to zero as a function of the domain-wall width parameter normalized by the Fermi wavelength. In the case of wall normal to $[\bar{1} 1 0]$, the grazing incidence channels cause a slower decay of R_r . Spin-orbit interaction is set to zero in this calculation, but all other parameters remain the same as in the calculations leading to a large value of R_r in Fig. 1. The value of λ_F is the same as in Fig. 1.

In order to gain further understanding of the physics underlying the DW resistance, we study the thick DW limit. We first consider the Bloch wall, for which magnetization is always perpendicular to the current, chosen here to flow along the $[100]$ direction. Owing to the symmetry of the zinc-blende structure, there is no anisotropic magnetoresistance (AMR) in such a case. The lack of AMR does not imply that the distribution of open channels in the reciprocal space is identical for all magnetization directions θ , where θ is the angle of \mathbf{M} with respect to the $[001]$ direction. We show now that the dependence of this distribution on θ gives rise to DWR in the adiabatic limit. To this end we use the adiabatic transport model, defined as follows. We consider all \mathbf{k} vectors for which carrier propagation for given spatially uniform $\mathbf{M}(\theta)$ and Fermi level is possible. We project these vectors on a plane perpendicular to the current direction, obtaining a 2D closed area $S(\theta)$ in the reciprocal space. Next, we turn the magnetization by a small angle and form the projection again, keeping constant h_0 , E_F , and the tunneling direction. For each step, the corresponding $S(\theta)$ is different, reflecting the rotation of \mathbf{M} , and the coupling between the spin and orbital degrees of freedom. Finally, after rotating the magnetization through the half-circle, we find a common subset of all $S(\theta)$ for

$0 \leq \theta \leq \pi$, by retaining only these channels that are open for all θ . This approach is a generalization of a qualitative model presented in Ref. [7]. However, we do not use the spherical approximation for the bands, so that an $S(\theta)$ for a general θ cannot be obtained by a simple rotation of $S(0)$.

In Fig. 3, we present the total DW resistance (in the units of R_s) as a function of θ , which is determined from the common subset $S_c(\theta)$ of areas S corresponding to all relevant subbands and magnetization angles up to θ , and $S(0)$ yields the Sharvin resistance R_s . We find a very good agreement between the calculated resistance of the thick Bloch DW and the one obtained in the adiabatic model. A direct inspection of transmission coefficients reveals that the distribution of open channels is very similar in both approaches. To verify our arguments we consider a 90° DW. We find good agreement between the calculated value of DWR and the one from the adiabatic model for $\theta = 90^\circ$, see Fig. 3.

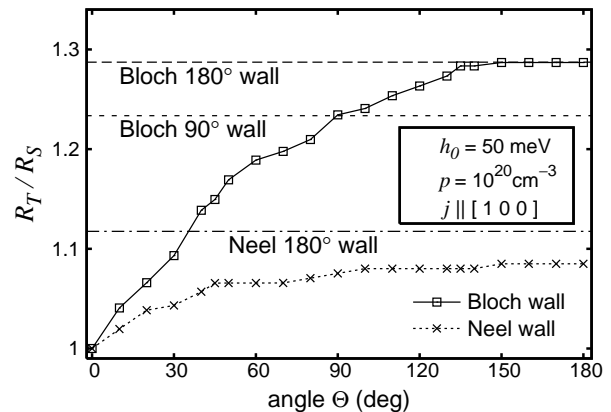


FIG. 3: Total resistance normalized by the Sharvin resistance, R_T/R_S , calculated within the adiabatic model as a function of the angle between the magnetization and $[001]$ direction for the Bloch and Néel walls. Horizontal lines show R_T/R_S computed within the full model in the adiabatic limit ($\lambda_W/\lambda_F = 1.4$) for three types of walls.

It is known that $(\text{Ga,Mn})\text{As}$ films reveal resistance anisotropy when magnetization is tilted towards the current direction.^{6,18} The above reasoning, however, remains unchanged for the case of the Néel wall, and the magnitudes of DWR can be obtained in the same way. In agreement with the results discussed above (see Fig. 1(a)), we find that more channels are left open after rotating \mathbf{M} by π in the xz plane (Néel DW) than in the zy plane (Bloch wall).

The values of DWR calculated from the adiabatic and the exact model for the 180° Néel wall differ somewhat more than in the case of the Bloch DW, see Fig. 3. This difference is caused by grazing incidence channels, for which the energy-integrated transmission coefficients are, on average, much smaller than the ones in the case of the Bloch DW.

In the limit of vanishing spin-orbit splitting, shapes

and orientations of the areas S are identical for all θ values. Therefore, their common subset is equal to $S(0)$ and, hence, to the Sharvin resistance R_S . Thus DWR vanishes totally in the adiabatic approximation. However, when the DW thickness decreases, a gradual closing of the tunneling channels takes place. Accordingly, the magnitude of R_T , calculated within the exact model grows exponentially, when λ_W/λ_F decreases (Fig. 2).

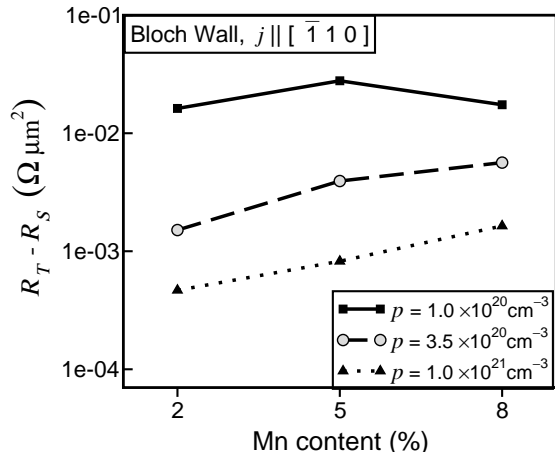


FIG. 4: Predicted values of the domain-wall resistance in the adiabatic limit for various hole concentrations. The data are for the saturation value of spin-splitting at a given Mn concentration x .

An important question arises whether the adiabatic DWR discussed here could explain experimental magnitudes of DWR in (Ga,Mn)As. Figure 4 shows the values of the intrinsic DWR, i.e., $R_T - R_S$ in the adiabatic limit for experimentally relevant ranges of the

hole concentrations and Mn densities. The computed values of DWR are positive. The sign of the effect is in disagreement with the findings of Tang *et al.*,² who reported a negative value of DWR for their samples of (Ga,Mn)As. By contrast, Chiba *et al.*³ found a positive value, $\text{DWR} = 0.5 \pm 0.1 \Omega \mu\text{m}^2$ for $p \approx 2 \times 10^{20} \text{ cm}^{-3}$ and $x = 0.05$. A comparison of this experimental value with the results of Fig. 4 shows that the computed values are at least one order of magnitude smaller. We recall at this point that high hole and Mn concentrations, necessary to observe the ferromagnetism, result in a short mean free path in these systems, typically much smaller than the DW width.

In conclusion, according to the detailed quantitative studies presented here, the spin-orbit interaction leads to a non-zero value of domain-wall resistance even in the adiabatic limit. The magnitude of this adiabatic resistance depends significantly on the character of the domain-wall and its crystallographic orientation. However, the sign and magnitude of the computed results are in variance with the recent experimental results for (Ga,Mn)As. We take this disagreement as an evidence for the paramount importance of disorder effects in the physics of DWR in carrier-controlled ferromagnetic semiconductors. However, non-zero domain-wall resistance induced by spin-orbit interactions can presumably be detected in those ferromagnetic systems, in which both coherence length and mean free path are longer than the domain-wall width.

We thank P. Kacman, H. Ohno, and P. Sankowski for valuable discussions. This work was partly supported by EU NANOSPIN project (EC:FP6-2002-IST-015728). R.O. acknowledges an additional support by Nicolaus Copernicus University Grant 381-F.

-
- ¹ M. Yamanouchi, D. Chiba, F. Matsukura, and H. Ohno, *Nature* **428**, 539 (2004); M. Yamanouchi, D. Chiba, F. Matsukura, T. Dietl, and H. Ohno, *Phys. Rev. Lett.* **96**, 096601 (2006).
 - ² H. X. Tang, S. Masmanidis, R. K. Kawakami, D. D. Awschalom, and M. L. Roukes, *Nature* **431**, 52 (2004).
 - ³ D. Chiba, M. Yamanouchi, F. Matsukura, T. Dietl, and H. Ohno, *Phys. Rev. Lett.* **96**, 096602 (2006).
 - ⁴ T. Dietl, H. Ohno, F. Matsukura, J. Cibert, and D. Ferrand, *Science*, **287**, 1019 (2000).
 - ⁵ T. Dietl, H. Ohno, and F. Matsukura, *Phys. Rev. B* **63**, 195205 (2001).
 - ⁶ T. Jungwirth, J. Sinova, J. Masek, J. Kucera, and A. H. MacDonald, *Rev. Mod. Phys.*, in press; cond-mat/0603380.
 - ⁷ Anh Kiet Nguyen, R. V. Shchelushkin, and A. Brataas, cond-mat/0601436.
 - ⁸ G. G. Cabrera and L. M. Falicov, *phys. stat. sol. (b)* **61**, 539 (1974);
 - ⁹ P. Van Dorpe, W. Van Roy, J. De Boeck, G. Borghs, P. Sankowski, P. Kacman, J. A. Majewski, and T. Dietl, *Phys. Rev. B* **72**, 205322 (2005).
 - ¹⁰ P. Sankowski, P. Kacman, J. A. Majewski, and T. Dietl, cond-mat/0509629, *Physica E* (2006), in press.
 - ¹¹ A. Di Carlo, P. Vogl, and W. Pötz, *Phys. Rev. B* **50**, 8358 (1994).
 - ¹² J. Okabayashi, A. Kimura, O. Rader, T. Mizokawa, A. Fujimori, T. Hayashi, and M. Tanaka *Physica E* **10**, 192 (2001).
 - ¹³ A. di Carlo and P. Lugli, *Semicond. Sci. Technol.* **10**, 1673 (1995).
 - ¹⁴ P. Kacman, *Semicond. Sci. Technol.* **16** R25, (2001).
 - ¹⁵ A. Hubert and R. Schäfer, (*Magnetic Domains : The Analysis of Magnetic Microstructures*, 1st ed. Springer, 2001).
 - ¹⁶ Supriyo Datta, *Electronic Transport in Mesoscopic Systems*, (Cambridge University Press, Cambridge, 1995).
 - ¹⁷ J. F. Gregg, W. Allen, K. Ounadjela, M. Viret, M. Hehn, S. M. Thompson, and J. M. D. Coey, *Phys. Rev. Lett.* **77**, 1580, (1996); P. Levy and S. Zhang, *Phys. Rev. Lett.* **79**, 5110 (1997).
 - ¹⁸ D. V. Baxter, D. Ruzmetov, J. Scherschligt, Y. Sasaki, X. Liu, J. K. Furdyna, and C. H. Mielke, *Phys. Rev. B* **65**, 212407 (2002).